

## Continuum Model for Low Temperature Relaxation of Crystal Steps

O. Pierre-Louis

*Laboratoire de Spectrométrie Physique-Grephe, CNRS, UJF-Grenoble 1, BP87, F38402 Saint Martin d'Hères, France*  
(Received 4 January 2001; published 21 August 2001)

High and low temperature relaxation of crystal steps are described in a unified picture, using a continuum model based on a modified expression of the step-free energy. Results are in agreement with experiments and Monte Carlo simulations of step fluctuations and monolayer cluster diffusion and relaxation. In an extended model where mass exchange with neighboring terraces is allowed, step transparency and a low temperature regime for unstable step meandering are found.

DOI: 10.1103/PhysRevLett.87.106104

PACS numbers: 68.35.Fx, 05.40.-a, 61.46.+w, 66.30.Qa

The upsurge of nanotechnologies and of microscopic visualization techniques (such as scanning tunneling microscopy) in the past 15 years raises the challenge for modeling crystal surfaces morphology at smaller and smaller scales. Surface dynamics crucially depends on the underlying microscopic discreteness, especially in nonequilibrium or low temperature conditions. Accounting for the presence of crystal steps has allowed some important breakthroughs in the description of growth and relaxation of nanostructures [1,2]. In this Letter, it is pointed out that steps themselves exhibit a discrete substructure that drastically affects their dynamics at low temperatures, and that a continuum model based on a modified free energy allows one to account for this low temperature regime.

An isolated step is always rough: Steps do not have macroscopic facets or sharp angles (see Ref. [2] for a discussion). This statement has motivated a modeling for mass transport along steps (edge diffusion), first developed by Mullins [3], based on a description at length scales larger than the distance between kinks. Measurement of the time correlations of fluctuating steps [4] has revealed a low temperature regime for edge diffusion not explained by this model. Systematic low temperature deviations from its predictions have also been reported in experimental and kinetic Monte Carlo (MC) studies of monolayer island diffusion [5,6], and relaxation from a deformed shape [7].

In the following, a continuum model is presented, based on a modified expression of the step-free energy that explicitly accounts for edge atoms (i.e., mobile atoms at the steps). This model exhibits high and low temperature regimes in agreement with kinetic MC simulations and experiments. When mass exchange with neighboring terraces is allowed, it also accounts for the recently observed step transparency (also called permeability) on high temperature Si(111) surfaces [8], and for low temperature wavelength selection of unstable step meandering during growth [9].

The free energy of a step is traditionally taken to be proportional to its length [2]:

$$\mathcal{F}_0 = \int dx \gamma [1 + (\partial_x \zeta)^2]^{1/2}, \quad (1)$$

where  $\zeta(x, t)$  is the meander of the step with respect to the straight step configuration, and  $\partial_x$  denotes the partial derivation with respect to  $x$ . At low temperatures, one can neglect atom detachment from steps to terraces [4]. Mass transport then occurs only via mobile edge-atom diffusion along the step edge, and is driven by gradients of the chemical potential  $\mu = \Omega(\delta \mathcal{F}_0 / \delta \zeta) = \Omega \tilde{\gamma} \kappa$ , where  $\Omega$  is the atomic area,  $\delta / \delta \zeta$  denotes a functional derivative with respect to  $\zeta$ , and  $\tilde{\gamma} = \gamma + \gamma''$  is the step stiffness. Step motion results from the divergence of the local mass flux  $j = -a D_L \partial_x \mu / k_B T$ , where  $D_L$  is the macroscopic diffusion constant for mass transport along the step. Thus,

$$\partial_t \zeta = \partial_x \left[ \frac{a D_L}{k_B T} \partial_x (\Omega \tilde{\gamma} \kappa) \right]. \quad (2)$$

Equation (2) is the usual starting point for studies of edge diffusion-driven step dynamics. It is always valid for length scales larger than the distance between kinks, and long enough time scales.

As an example, let us consider a [110] step on a Cu(100) surface, where the kink energy is  $E_k = 0.13$  eV [4]. At low temperatures, kink density is  $N_k \approx 2 \exp(-E_k / k_B T) / a$ , where  $a$  is the lattice spacing. The distance between kinks is then  $N_k^{-1} \approx 75a$  for  $T = 300$  K, and  $N_k^{-1} \approx 10^3 a$  at  $T = 200$  K. Hence, not only  $N_k^{-1} \gg a$ , but at low enough  $T$ ,  $N_k^{-1}$  may be much larger than observation length scales: Scanning tunneling microscopy nowadays allows one to study step fluctuations up to atomic scales [4,10], and monolayer clusters of several nanometers are observed [6]. Moreover, step relaxation time scales related to edge-atom motion from kink to kink can also become large when  $N_k$  is small.

The very different role played by mobile edge atoms and atoms incorporated into the solid suggests that the step should rather be described as a heterogeneous phase at scales smaller than  $N_k^{-1}$ . Hence, the total free energy shall be written as

$$\mathcal{F} = \int dx \left[ \gamma [1 + (\partial_x \zeta)^2]^{1/2} + \frac{\alpha}{2} (c - c_{\text{eq}}^0)^2 \right], \quad (3)$$

for a step wandering about the closed-packed orientation  $\hat{x}$ .  $c(x, t)$  is the macroscopic concentration of mobile edge atoms along the step, as presented in Fig. 1. The term  $(c - c_{\text{eq}}^0)^2$  accounts for the departure from local equilibrium, and will be seen to be irrelevant at high temperature. We shall see, in the following, how step relaxation based on Eq. (3) accounts for high and low  $T$  regimes in a wide variety of physical situations. Kinks are not explicitly described in this model. Nevertheless, the relaxation of  $c$  to its equilibrium value  $c_{\text{eq}}^0$  implicitly involves the kink distribution, as will be seen later.

For small perturbations, Eq. (3) is expanded to second order in  $\zeta$  and  $u = c - c_{\text{eq}}^0$ . At thermal equilibrium, equipartition implies that each Fourier mode  $u_k$  or  $\zeta_k$  of wave vector  $k$  carries the same amount of energy:

$$\frac{\tilde{\gamma}}{2} k^2 \langle |\zeta_k|^2 \rangle = \frac{\alpha}{2} \langle |u_k|^2 \rangle = \frac{k_B T}{2}. \quad (4)$$

As a first mean field approximation, edge atoms can be considered as noninteracting; thus  $\langle |u_k|^2 \rangle = c_{\text{eq}}^0$  [11], and  $\alpha = k_B T / c_{\text{eq}}^0$ .

Let us now turn to the dynamics. In a way similar to model C in critical phenomena [12], two evolution equations are written. The first one for the nonconserved step position  $\zeta$  reads

$$\frac{\partial_t \zeta}{\Omega} = -A \frac{\delta \mathcal{F}}{\delta \zeta} + \eta, \quad (5)$$

where  $A$  is a kinetic coefficient, and  $\eta$  is a Langevin force. A second evolution equation is written for the conserved total concentration of atoms (i.e., atoms in the solid and edge atoms)  $\psi = \zeta / \Omega + c$ :

$$\partial_t \psi = \partial_x \left[ B \partial_x \left( \frac{\delta \mathcal{F}}{\delta \psi} \right) - q \right], \quad (6)$$

where  $B$  is a mobility, and  $q$  is a conserved noise. Using Eq. (3) in Eqs. (5) and (6), a set of coupled evolution equations is found:

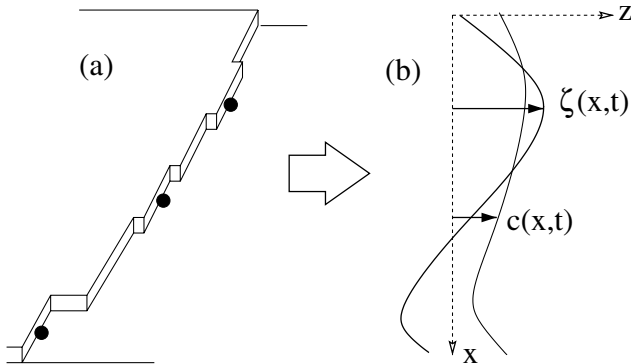


FIG. 1. The step position  $\zeta(x, t)$  and the macroscopic edge-atom concentration  $c(x, t)$  are both needed in a continuum description for low temperature dynamics of crystal steps.

$$\frac{\partial_t \zeta}{\Omega} = \nu(c - c_{\text{eq}}) + \eta, \quad (7)$$

$$\partial_t c = \partial_x [B \partial_x c - q] - \nu(c - c_{\text{eq}}) - \eta, \quad (8)$$

where  $\nu = A\alpha$ , and  $c_{\text{eq}}$  is found to obey a Gibbs-Thomson relation:

$$c_{\text{eq}} = c_{\text{eq}}^0 (1 + \Gamma \kappa), \quad (9)$$

where  $\kappa$  is the step curvature, and  $\Gamma = \Omega \tilde{\gamma} / k_B T$  is the capillary length. The obtained evolution equations share similarities with models of Refs. [13–15]. Nevertheless, these were not derived from the free energy  $\mathcal{F}$ . As mentioned by these authors, the model [(7) and (8)] leads to a crossover between two regimes for step relaxation. In the following, a detailed analysis of step-atom kinetics is performed, which leads to quantitative predictions.

Following Ref. [16], the correlations of the Langevin forces are found within a local thermodynamic equilibrium approximation:

$$\langle \eta(x, t) \eta(x', t') \rangle = 2\nu c(x, t) \delta(x - x') \delta(t - t'), \quad (10)$$

$$\langle q(x, t) q(x', t') \rangle = 2Bc(x, t) \delta(x - x') \delta(t - t').$$

As a first approach, we now propose some phenomenological expressions for the kinetic coefficients. The macroscopic diffusion constant of edge atoms along the steps is approximated by that of a tracer edge atom on a frozen step with a given kink density  $N_k$ . Defining the diffusion constant of mobile edge atoms between kinks  $D$  and the kinetic attachment lengths  $d_{\pm} = a[\exp(E_{\pm}/k_B T) - 1]$ , where  $E_{\pm}$  are the additional energy barrier (with respect to diffusion) for atoms to stick to a kink from both sides, and using the result of Ref. [17], it is found that

$$B = \frac{D}{1 + N_k(d_+ + d_-)}. \quad (11)$$

The macroscopic attachment coefficient  $\nu$  is the inverse of the relaxation time of the concentration, which is related to the time scale of diffusion of a mobile atom from one kink to another. Hence,

$$\nu \approx BN_k^2. \quad (12)$$

We shall first address the case of a straight step at equilibrium fluctuating about the close-packed direction  $x$ . The time correlation function,

$$G(t) = \langle [\zeta(x, t) - \zeta(x, t + \tau)]^2 \rangle, \quad (13)$$

has been measured in experiments and MC simulations [4]. This quantity is evaluated within the quasistatic approximation, which stipulates that the edge-atom concentration reaches a steady state on time scales much shorter than kink motion. Thus, the left-hand side of Eq. (8) vanishes. Comparing the quasistatic and full dispersion relations as in Ref. [18], and using Eq. (12), the quasistatic approximation is found to be valid when

$$\Gamma a^2 c_{\text{eq}}^0 \ll N_k^{-2} + k^{-2}. \quad (14)$$

At low  $T$ , in a simple bond-counting model and for a step along a high symmetry orientation,  $\Gamma a^2 c_{\text{eq}} \sim a^2 \exp(-E_k/k_B T) \ll N_k^{-2} \sim a^2 \exp(2E_k/k_B T)$ , where  $E_k$  is the kink energy. At high  $T$ ,  $c_{\text{eq}}^0 \sim 1/a$ ,  $N_k \sim a^{-1}$ , and  $\Gamma \rightarrow 0$ . Hence, the quasistatic limit is valid at all  $T$ .

Linearizing Eqs. (7) and (8), in the quasistatic limit,  $G(t)$  is easily evaluated. For large observation time scales, long wavelength fluctuations  $\lambda \gg N_k^{-1}$  dominate, and

$$G_{\text{long}}(\tau) = \frac{a^2 \Gamma(3/4)}{\pi} (b^2)^{3/4} (B c_{\text{eq}}^0)^{1/4} \tau^{1/4}, \quad (15)$$

where  $b^2 = ak_B T / \tilde{\gamma}$  is the step diffusivity. This expression corresponds to the one given in Ref. [19] starting from the Mullins model Eq. (2), with  $D_L = a B c_{\text{eq}}^0$  as expected from Ref. [3]. For short observation time scales, only short wavelengths ( $\lambda \ll N_k^{-1}$ ) contribute to  $G$ , and

$$G_{\text{short}}(\tau) = \frac{a^{3/2}}{\sqrt{\pi}} (\nu c_{\text{eq}}^0 b^2)^{1/2} \tau^{1/2}. \quad (16)$$

Using Eq. (12) and the relation  $b^2 \sim N_k$ , valid at low  $T$ , the crossover between the two regimes is found to correspond to  $G(t) \sim a^2$ . This result was found by Giesen *et al.* [4], by means of a discrete random kink model and MC simulations. From the relation  $G(t^*) \sim a^2$ , the crossover time between the two regimes is found to be

$$t^* \sim (N_k^3 a^2 B c_{\text{eq}}^0)^{-1}. \quad (17)$$

Thus, the criterion of validity of Eq. (2) is  $t \gg t^*$ . Using numerical values for Cu(11n) vicinal surfaces given in Ref. [4], one finds  $t^* \sim 10^{-19} \exp(14870/T)$  s, where  $T$  is in kelvin. With observation times  $t^* \sim 1$  s [4], the crossover is found for  $T \approx 340$  K, in quantitative agreement with experiments [4].

Monolayer cluster relaxation and diffusion might also be addressed by this model. Let us consider a circular island having small perturbations about its mean radius  $R_0$  defined by  $R(\theta) = R_0 + \rho(\theta)$ . The polar coordinates  $R$  and  $\theta$  are used. In a ‘‘circular model,’’  $x$  is simply replaced in the model by  $R_0 \theta$  for small perturbations. In the linear approximation, the relaxation time of a small perturbation  $\rho = \epsilon \cos(n\theta)$  is

$$t_n = 2\pi \frac{R_0^2}{\nu \Gamma a^2 c_{\text{eq}}} \frac{n^2 + R_0^2(\nu/B)}{n^2(n^2 - 1)}. \quad (18)$$

A crossover from  $t_r \sim R_0^4$  when  $R_0 \gg N_k^{-1}$  to  $t_r \sim R_0^2$  when  $R_0 \ll N_k^{-1}$  is found in agreement with kinetic MC simulations in Ref. [7].

The divergence of  $t_1$  comes from the translational invariance of the cluster position: It costs no energy to move the cluster as a whole ( $n = 1$  mode). Thus, random motion of atoms along the periphery will cause diffusion of the cluster, with diffusion constant (calculated without using the quasistatic limit):

$$D_c = \frac{\langle \mathbf{r}_{\text{c.m.}}^2(t) \rangle}{4t} = \frac{a^4 c_{\text{eq}}}{\pi R_0} \frac{1}{R_0^2/B + 1/\nu}, \quad (19)$$

where  $\mathbf{r}_{\text{c.m.}}$  indicates the position of the center of mass of the cluster. The high  $T$  behavior  $D_c = a^3 D_L / \pi R_0^3$ , calculated from Eq. 2 in Refs. [18,20], is recovered when  $R_0 \gg N_k^{-1}$ , provided once again that  $D_L = a B c_{\text{eq}}^0$ . In the low  $T$  regime, where  $R_0 \ll N_k^{-1}$ , another scaling limit is found:  $D_c \sim R_0^{-1}$ , in agreement with previous experimental [6] or MC [5] studies. The circular approximation catches the essential physical point, which is the existence of orientations for which  $N_k^{-1}$  is much larger than the size of the cluster. Nevertheless, including anisotropy in our model is needed for a quantitative comparison with low  $T$  experiments and kinetic MC simulations.

At higher  $T$  or during growth, steps exchange mass with terraces. For low kink concentration  $N_k \ll a^{-1}$ , direct exchange from kink to terrace can be neglected, and step meandering is weak, i.e.,  $\partial_x \zeta \ll 1$ . An extended model may then be written, with Eqs. (7), (9), and

$$\partial_t c = \partial_x [B \partial_x c] - \nu(c - c_{\text{eq}}) + J_+ + J_-, \quad (20)$$

$$J_{\pm} = \beta_{\pm} C_{\pm} - \nu_{\pm} c, \quad (21)$$

$$\partial_t C = D_s \nabla^2 C + F - C/\tau, \quad (22)$$

where  $C$  is the concentration of adatoms on terraces.  $D_s$  is their diffusion constant,  $F$  the incoming flux on terraces, and  $\tau$  the adatom desorption time. Langevin forces were omitted in Eqs. (20)–(22) for the sake of clarity in this brief exposition.  $+$  and  $-$  designate the lower and the upper sides of the step, respectively,  $\nu_{\pm}$  and  $\beta_{\pm}$  are kinetic coefficients. At equilibrium  $c = c_{\text{eq}}^0$  and  $C = C_{\text{eq}}^0$ , and there should be no mass flux (detailed balance) so that  $J_+ = J_- = 0$ . Thus,  $C_{\text{eq}}^0/c_{\text{eq}}^0 = \nu_+/\beta_+ = \nu_-/\beta_-$ . Since we address the case of weak meandering, exchange mass fluxes between steps and terraces are given by  $J_{\pm} \approx -D_s \partial_z C_{\pm}$ , where  $z$  is defined in Fig. 1. These latter equations allow one to close the model and to evaluate the concentration.

In the case of slow diffusion along steps (i.e.,  $B$  small), or for long wavelength perturbations (larger than  $N_k^{-1}$ ), the first term in the right-hand side of Eq. (20) vanishes. If an additional approximation is made in taking the variations of the adatom concentration  $C$  on terraces to be much slower than the relaxation time  $(\nu + \nu_+ + \nu_-)^{-1}$  of the edge-atom concentration  $c$ , we can set  $\partial_t c = 0$  in Eq. (20). The resulting model may be written

$$\frac{1}{\Omega} \partial_t \zeta = D_s \partial_z C_+ - D_s \partial_z C_-, \quad (23)$$

$$D_s \partial_z C_{\pm} = \pm \tilde{\beta}_{\pm} (C_{\pm} - C_{\text{eq}}) + \beta_0 (C_+ - C_-), \quad (24)$$

$$C_{\text{eq}} = C_{\text{eq}}^0 (1 + \Gamma \kappa), \quad (25)$$

where effective kinetic coefficients are defined via  $\tilde{\beta}_+/\beta_+ = \tilde{\beta}_-/\beta_- = \nu/(\nu + \nu_+ + \nu_-)$ , and

$\beta_0 = \beta_+ \nu_- / (\nu_+ + \nu_-)$ . With Eqs. (22)–(25), we have obtained the standard [8] model for “transparent” steps as a special limit. Step transparency (i.e.,  $\beta_0 \neq 0$ ) is understood as the possibility for an atom to attach to a step from a terrace, and detach to the other terrace before reaching a kink. Transparency appears as a natural ingredient of the model Eqs. (7) and (20)–(22).

As a last remark, we shall calculate the most unstable wavelength for the meandering instability first addressed by Bales and Zangwill [21], with step relaxation provided by the full model Eqs. (20)–(22). We use the following parameters:  $\beta_- = 0$  and  $\nu_- = 0$  (i.e., no mass exchange with the upper terrace);  $C_{\text{eq}}^0 = 0$ ,  $\nu_+ = 0$ , and  $\beta_+ \rightarrow \infty$  (this implies  $C_+ = 0$ ). Moreover, desorption is taken to be vanishingly small:  $1/\tau = 0$ . The growth rate of a small in-phase perturbation  $\zeta(x, t) = \exp(i\omega t + ikx)\zeta_{\omega k}$  of all steps on a vicinal surface reads

$$i\omega = \frac{-k^4 \Gamma B C_{\text{eq}}^0 + F[k\ell \tanh(k\ell) + \text{sech}(k\ell) - 1]}{1 + (B/\nu)k^2}, \quad (26)$$

where  $\ell$  is the mean interstep distance. The most unstable wavelength is calculated in the long wavelength limit  $k\ell \ll 1$  (valid for small fluxes  $F$ ). One finds

$$\lambda_1 = 4\pi(\Gamma B C_{\text{eq}}^0 / F \ell^2)^{1/2}, \quad (27)$$

when  $N_k^{-1} \ll \lambda_1$ . In the opposite case  $N_k^{-1} \gg \lambda_1$ , a low  $T$  regime is found, where

$$\lambda_2 = 2^{1/4} \pi^{1/2} \lambda_1^{1/2} N_k^{-1/2}. \quad (28)$$

Using activation energies given in Ref. [4], one finds that  $\lambda_1$  and  $\lambda_2$  follow Arrhenius laws with activation energies 0.38 and 0.12 eV, respectively (within  $\sim 10\%$  error). The low  $T$  regime seems to provide the best fit to the experimental result of 0.09 eV [9]. It is not clear though how nonequilibrium line diffusion effects pointed out in Ref. [22] combine or compete with these results.

In conclusion, a model has been presented, based on Eqs. (3) and (12), that accounts both for high and low temperature step relaxation dynamics observed in experiments [4,6] and kinetic MC simulations [4,5]. When mass exchange with neighboring terraces is added to this model, step transparency appears as a natural consequence of a low kink density. We also point out a low temperature regime for step meandering during growth.

A systematic analysis from a microscopic theory is still needed for a more rigorous evaluation of the kinetic coefficients  $B$  and  $\nu$ . Moreover, numerical solution of the fully anisotropic model is needed in order to describe quantitatively monolayer cluster diffusion and relaxation.

Low temperature relaxation of three-dimensional clusters and nanostructures is a source of long-standing contro-

versies [2]. The basic difficulty comes from the singularity of the free energy for orientations in the vicinity of a facet. As opposed to this situation, the free energy of a step does not exhibit singularities. Thus, a direct generalization of the present study is not possible. Nevertheless, it provides some milestones for a continuum description of three-dimensional clusters [23] and nanostructures relaxation.

The author thanks T.L. Einstein for useful discussions and comments. This work was initiated at the University of Maryland, College Park, supported by NSF-MRSEC.

- 
- [1] W. K. Burton, N. Cabrera, and F. C. Frank, *Philos. Trans. R. Soc. London A* **243**, 299 (1951).
  - [2] A. Pimpinelli and J. Villain, *Physics of Crystal Growth* (Cambridge University Press, Cambridge, England, 1999).
  - [3] W. W. Mullins, *J. Appl. Phys.* **28**, 333 (1957); **30**, 77 (1959).
  - [4] M. Giesen-Seibert, F. Schmitz, R. Jentjens, and H. Ibach, *Surf. Sci.* **329**, 47 (1995).
  - [5] A. Bogicevic, S. Liu, J. Jacobsen, B. Lundqvist, and H. Metiu, *Phys. Rev. B* **57**, R9459 (1998).
  - [6] W. W. Pai, A. K. Swan, Z. Zhang, and J. F. Wendelken, *Phys. Rev. Lett.* **79**, 3210 (1997).
  - [7] P. Jensen, N. Combe, H. Larralde, J. L. Barrat, C. Misbah, and A. Pimpinelli, *Eur. Phys. J. B* **11**, 497 (1999).
  - [8] J.-J. Métois and S. Stoyanov, *Surf. Sci.* **440**, 407 (1999).
  - [9] T. Maroutian, L. Douillard, and H.-J. Ernst, *Phys. Rev. Lett.* **83**, 4353 (1999); (private communication).
  - [10] L. Kuipers, M. S. Hoogeman, and J. W. M. Frenken, *Phys. Rev. B* **52**, 11 387 (1995).
  - [11] L. D. Landau and E. M. Lifschitz, *Theoretical Physics V, Statistical Physics* (Pergamon, Oxford, 1967), Pt. 1, Sec. 113.
  - [12] P. C. Hohenberg and B. I. Halperin, *Rev. Mod. Phys.* **49**, 435 (1986).
  - [13] H. P. Bonzel and W. W. Mullins, *Surf. Sci.* **350**, 285 (1994).
  - [14] J. W. Cahn and J. E. Taylor, *Acta Metall. Mater.* **42**, 1045 (1994); R. E. Cafisch, Weinan E, M. F. Gyure, B. Merriman, and C. Ratsch, *Phys. Rev. E* **59**, 6879 (1999).
  - [15] S. V. Khare and T. L. Einstein, *Phys. Rev. B* **57**, 4782 (1998).
  - [16] O. Pierre-Louis and C. Misbah, *Phys. Rev. Lett.* **76**, 4761 (1996).
  - [17] A. Natori and R. W. Godby, *Phys. Rev. B* **47**, 15 816 (1993).
  - [18] O. Pierre-Louis and T. L. Einstein, *Phys. Rev. B* **62**, 13 697 (2000).
  - [19] N. C. Bartelt, J. L. Goldberg, T. L. Einstein, E. D. Williams, J. C. Heyraud, and J.-J. Métois, *Phys. Rev. B* **48**, 15 453 (1993).
  - [20] S. V. Khare, N. C. Bartelt, and T. L. Einstein, *Phys. Rev. Lett.* **75**, 2148 (1995); *Phys. Rev. B* **54**, 11 752 (1996).
  - [21] G. S. Bales and A. Zangwill, *Phys. Rev. B* **41**, 5500 (1990).
  - [22] O. Pierre-Louis, M. R. D’Orsogna, and T. L. Einstein, *Phys. Rev. Lett.* **82**, 366 (1999).
  - [23] N. Combe, P. Jensen, and A. Pimpinelli, *Phys. Rev. Lett.* **85**, 110 (2000).